Heterodyne near-field scanning optical microscopy with spectrally broad sources

Maxim Abashin,* Kazuhiro Ikeda, Robert Saperstein, and Yeshaiahu Fainman

Department of Electrical and Computer Engineering, University of California, San Diego, 9500 Gilman Drive, La Jolla, California 92093-0407, USA

**Corresponding author: mabashin@emerald.ucsd.edu*

Received December 2, 2008; revised March 2, 2009; accepted March 31, 2009; posted April 3, 2009 (Doc. ID 104804); published April 20, 2009

We propose to use low-coherence-length cw optical sources with a broad spectrum in heterodyne near-field scanning microscopy in order to imitate optical pulse propagation and to obtain information about spectrally variant properties of nanophotonic components. The dispersion difference in the interferometer arms for a symmetric acousto-optic modulator arrangement is shown to be negligible over appreciable bandwidths. Demonstration of the principle of operation and viability of this approach is provided by measurement of the group refractive index of a silicon channel waveguide. © 2009 Optical Society of America

OCIS codes: 030.1640, 180.4243, 230.7370.

Near-field scanning optical microscopy (NSOM) is a very popular technique for nanophotonics characterization [1–4]. With this method optical measurements are preformed with subwavelength spatial resolution by locally probing evanescent and propagating fields in the near-field region using a scanning tip with a nanoscale aperture. Heterodyne detection schemes can also be implemented in near-field microscopy to provide information about the optical amplitude and optical phase distribution, allowing more detailed descriptions of the measured device parameters [5–7]. Another advantage of the heterodyne detection approach is the coherent gain attributable to measuring the interference term between a weak near-field signal and a strong reference field.

Mode-locked lasers are commonly used to study ultrashort pulse propagation phenomena in nanophotonic devices. Indirect characterization has been performed by studying spectral evolution as the light propagates through the device [8], and direct tracking of ultrashort optical pulses using heterodyne detection can also be implemented [9]. Since the detection process commonly used in this cross-correlation approach is slow compared to the repetition rate of the mode-locked laser source, the amplitude images obtained at a particular delay time do not represent a snapshot corresponding to a single pulse, but rather an average through a large number of pulses. The finite spatial extent of the imaged ultrashort pulses is achieved owing to the small coherence length of ultrashort pulses. Therefore, when instantaneous or nonlinear responses of the nanophotonic device are not a concern, sources other than ultrashort pulse lasers that possess low coherence properties can be used. Since the coherence length of an optical field is inversely proportional to the spectral bandwidth of the source, in this Letter we propose for what is believed to be the first time to characterize wide-spectral-range properties of nanophotonic devices using broad-spectrum cw sources. This approach has several advantages over the ultrafast pulse implementation: reduced cost; smaller equipment size, weight, and power consumption; improved stability; and lower peak optical power, which can reduce nonlinear interactions in the sample under investigation and in the measurement system while preserving the same signal-to-noise ratio of the heterodyne measurements.

The heterodyne NSOM (HNSOM) we use in our experiments (Fig. 1) is similar to that described in [7], with the exception that in our current configuration the acousto-optic modulators (AOMs) are placed in the different arms of the Mach–Zehnder arrangement. The two AOMs are driven by rf signals of 40 MHz and 40.07 MHz, respectively, introducing a difference in the optical carrier frequencies of 70 kHz. The 70 kHz rf signal is also used as a reference for lock-in detection. This arrangement helps to minimize dispersion differences in the two arms of the Mach–Zehnder interferometer and prevents spectral phase distortion, which would result in decreased detection efficiency [10] and measurement accuracy. We use an Opto-Link OLSLD-15-HP4 superluminescent diode (SLD) as an optical source operating in the near-IR region at a center wavelength of $\lambda_c = 1539$ nm, FWHM of the spectrum, $\Delta\lambda = 44.5$ nm, and output optical power of $P_{out} = 30$ mW. Figure 2(a) shows the measured power spectrum of the SLD source.

To estimate the influence of unbalanced dispersion due to the possible difference in dispersive properties in the two arms of the Mach–Zehnder interferometer, we perform temporal cross-correlation by fixing the tip position in contact with an optical waveguide and

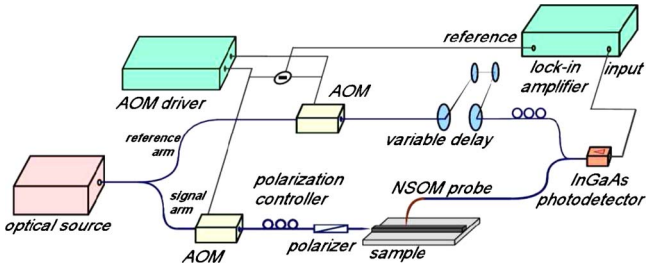

Fig. 1. (Color online) Heterodyne NSOM setup with symmetrical AOM arrangements.

0146-9592/09/091327-3/$15.00

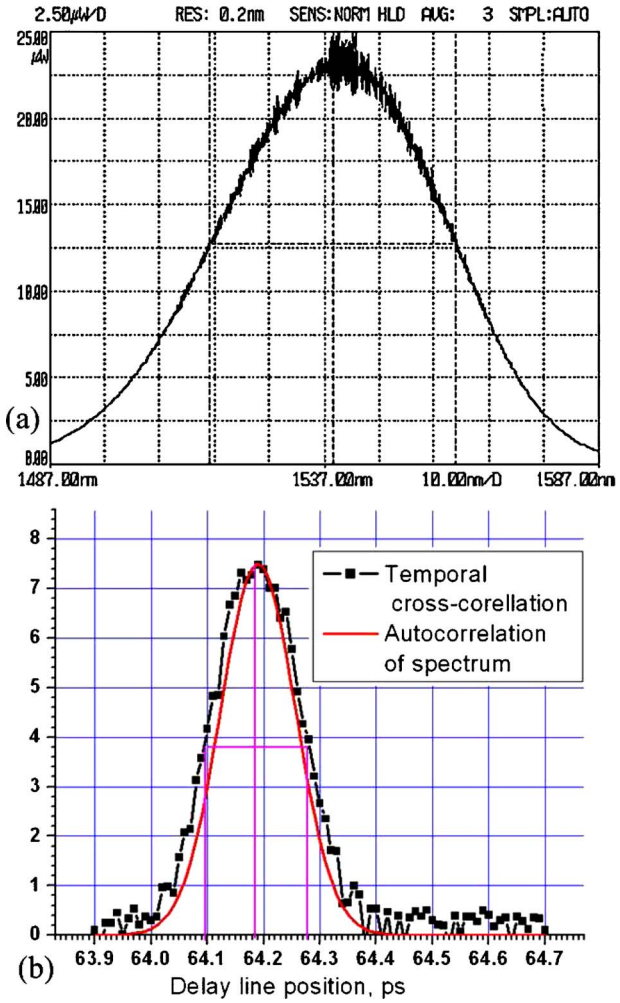

Fig. 2. (Color online) (a) Optical spectrum of SLD. (b) Temporal cross correlation of this source obtained in the HNSOM setup by varying delay line position with fixed probe position. Autocorrelation of spectral data is also shown for comparison.

scanning the variable delay line [see Fig. 2(b)]. The FWHM of temporal cross correlation estimated from this measurement is $\Delta\tau = 180$ fs. This result is very close to the theoretical limit in the absence of dispersion, which can be obtained by calculating the autocorrelation of spectral data from Fig. 2(a). This autocorrelation peak, obtained using Matlab's fast Fourier transform, has an FWHM of $\Delta\tau_{\text{spectr}} = 160$ fs. The ~10% broadening factor is tolerable for these measurements and is partially attributable to the optical waveguide used. The loss of accuracy owing to correlation trace broadening is neglected here but may need to be considered for measurements using very large optical bandwidths. For a fixed delay line position we scan the near-field probe to obtain NSOM image that represents spatial cross correlation of the broadband source in the photonic structure. In general, for a linear system/device under investigation in our HNSOM system, the measured output correlation functions should be the same using either a broad-bandwidth light source such as an SLD or a transform-limited ultrashort laser pulse of identical bandwidth (i.e., corresponding to pulse of about 180 fs), provided the dispersion in the two arms of the Mach–Zehnder arrangement in the absence of the system/device is identical. A typical measured near-field image for a silicon channel waveguide device is shown in Fig. 3. It should be noted that near-field images obtained using broad-bandwidth sources also look "cleaner" than those obtained using a tunable cw narrow line sources, because undesirable light paths that exceed the coherence length of the source with respect to the reference path do not contribute to the image. This is an additional advantage of our method, because it decreases the detected values of the spatial field distributions that correspond to "spatial" noise (e.g., stray light due to inefficient coupling to the nanophotonic circuit), thereby improving the signal-to-noise ratio of the detected near-field images.

Using the HNSOM system described above, we perform a demonstration experiment by measuring the group index of a silicon-on-insulator (SOI) channel waveguides. The sample consists of an L-shaped silicon channel waveguide with height $h = 250$ nm and width $w = 700$ nm. The input and output facets of the waveguide are cleaved and TM-polarized light (E-field perpendicular to the SOI wafer plane) is coupled into the waveguide under investigation using OZ Optics polarization-maintaining lensed fiber. A series of HNSOM amplitude distribution images are taken for a number of time delays set by the variable delay line. The results showing integrated amplitude in the waveguide for different delays are presented in Fig. 4(a). Next, we process the information on this image by finding the positions of the peaks and plotting the distance traveled by the correlation peak versus time [Fig. 4(b)]. By fitting the data set with a linear equation, we derive the group velocity. The group index of the waveguide is determined as $n_{\text{gr}} = c/v_{\text{gr}}$, where c is the speed of light in vacuum and v_{gr} is the obtained group velocity. From the linear fitting we get $v_{\text{gr}} = 68.78 \pm 2.95$ μm/ps and thus $v_{\text{gr}} = 4.36 \pm 0.19$. It is worth noticing that the found value is higher than the phase (effective) refractive index

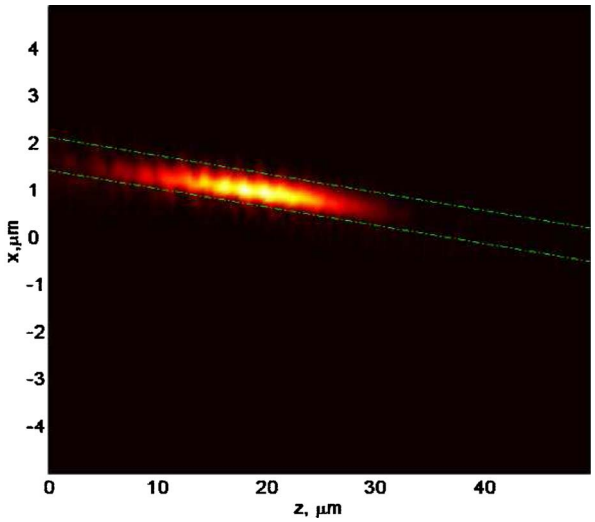

Fig. 3. (Color online) Example of near-field amplitude image obtained in HNSOM setup with broad-spectrum optical source. Approximate boundaries of waveguide from topography image are shown with dashed lines.

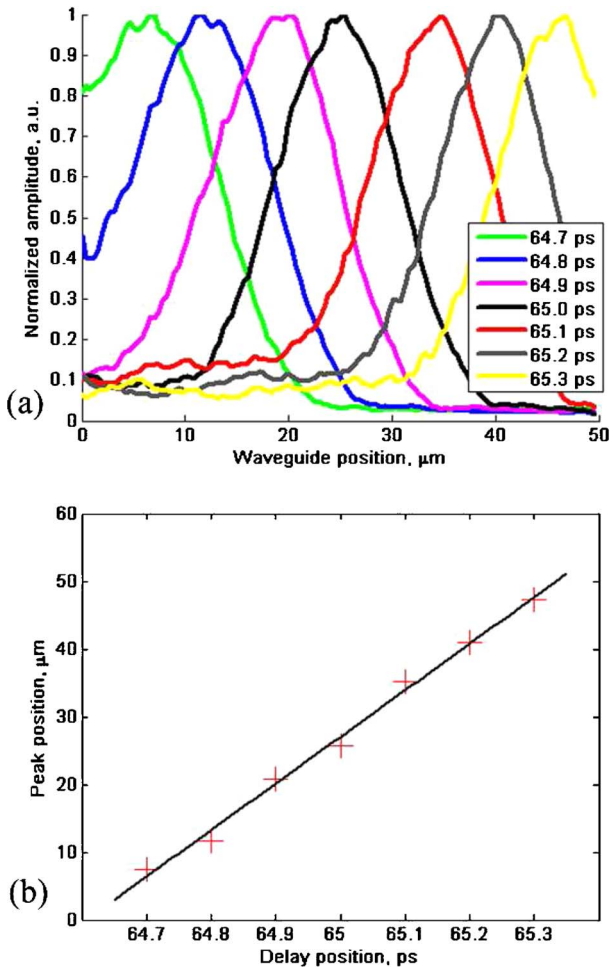

Fig. 4. (Color online) (Color online) (a) Optical amplitude over the waveguide length for different positions of the delay line. (b) Positions of the amplitude maxima and their linear fitting.

for this waveguide and even higher than the material refractive index for bulk silicon. This occurs due to the waveguide dispersion and negative derivative of the effective refractive index with respect to wavelength: $v_{gr}=(n_{eff}-\lambda)(dn_{eff}/d\lambda)$. We also used the beam propagation method mode solver from RSoft to calculate the effective indices at wavelengths around the λ_c. Implementing a simple two-point estimation of the derivative we get a numerical estimation of $v_{gr}=4.39\pm0.03$ within a FWHM band of λ_c. The averaged effective refractive index $n_{eff}=2.3\pm0.1$ found from the HNSOM phase distribution is also close to the numerically obtained $n_{eff}=2.13$ calculated for λ_c. In general, the values for the group index in SOI waveguides are strongly dependent on the waveguide geometry and wavelength, and as evident from the results reported in [11–14], the group indices for waveguides with similar geometries vary between 4 and 5. The errors of our near-field index characterization can be decreased by taking higher-resolution images and by using a higher-precision variable delay line. Our current image pixel size is approximately 470 nm, whereas the probe's aperture, and thus the approximate spatial resolution limit, is 200 nm; in addition the documented accuracy of the delay line used in our setup is ±0.02 ps.

In conclusion, we have shown that broad-spectrum cw light sources possessing a low coherence length can be used in HNSOM experiments to characterize the spectrally variant properties of photonic structures such as pulse propagation in a waveguide. This approach provides a low-cost and flexible solution for enhancing near-field characterization where previously mode-locked lasers have been required. In photonic circuits with multiple elements, the measurement localization intrinsic to low-coherence HNSOM can be utilized to find the group index for each component. Potentially this characterization method can be enhanced by analyzing the cross-correlation shape evolution and by the studying optical phase data readily available in HNSOM measurements. To demonstrate the applicability, we measured the group index of an SOI channel waveguide using this technique. The obtained value of the group index $n_{gr}=4.36\pm0.19$ was a close match with the numerically calculated parameter $n_{gr}=4.39\pm0.03$.

This work was supported by the Defense Advanced Research Projects Agency (DARPA), the National Science Foundation (NSF), the NSF Center for Integrated Access Networks Engineering Research Center, the U.S. Air Force Office of Scientific Research (AFOSR), and the U.S. Army Research Office (ARO).

References

1. V. S. Volkov, S. I. Bozhevolnyi, P. I. Borel, L. H. Frandsen, and M. Kristensen, Phys. Rev. B **72**, 035118 (2005).
2. M. Abashin, P. Tortora, I. Märki, U. Levy, W. Nakagawa, L. Vaccaro, H. Herzig, and Y. Fainman, Opt. Express **14**, 1643 (2006).
3. B. Cluzel, E. Picard, T. Charvolin, E. Hadji, L. Lalouat, F. de Fornel, C. Sauvan, and P. Lalanne, Appl. Phys. Lett. **88**, 051112 (2006).
4. R. Yan, G. Yuan, R. Pownall, and K. L. Lear, *Lasers and Electro-Optics Society, The 20th Annual Meeting of the IEEE* (IEEE, 2007), pp. 543–544.
5. M. L. M. Balistreri, J. P. Korterik, L. Kiupers, and N. F. van Hulst, J. Lightwave Technol. **19**, 1169 (2001).
6. A. Nesci, R. Dändliker, and H. Herzig, Opt. Lett. **26**, 208 (2001).
7. A. Nesci and Y. Fainman, Proc. SPIE **5181**, 62 (2003).
8. J. D. Mills, T. Chaipiboonwong, W. S. Brocklesby, M. D. B. Charlton, C. Netti, M. E. Zoorob, and J. J. Baumberg, Appl. Phys. Lett. **89**, 051101 (2006).
9. M. L. M. Balistreri, H. Gersen, J. P. Korterik, L. Kuipers, and N. F. van Hulst, Science **294**, 1080 (2001).
10. H. Gersen, J. P. Korterik, N. F. van Hulst, and L. Kuipers, Phys. Rev. E **68**, 026604 (2003).
11. E. Dulkeith, F. Xia, L. Schares, W. M. J. Green, and Y. A. Vlasov, Opt. Express **14**, 3853 (2006).
12. A. Sakai, G. Hara, and T. Baba, Jpn. J. Appl. Phys. Part 2 **40**, L383 (2001).
13. C. Turner, C. Manolatou, B. S. Schmidt, M. Lipson, M. A. Foster, J. E. Sharping, and A. L. Gaeta, Opt. Express **14**, 4357 (2006).
14. J. Jágerská, N. Le Thomas, R. Houdré, J. Bolten, C. Moormann, T. Wahlbrink, J. Čtyroký, M. Waldow, and M. Först, Opt. Lett. **32**, 2723 (2007).